

## Original Article

# Development of a benzene-induced AML model in CBA/Ca mice with bone marrow immunophenotypic features

Jin He<sup>1,2</sup>, Shaolei Zang<sup>1</sup>, Min Ji<sup>1</sup>, Daoxin Ma<sup>1</sup>, Chunyan Ji<sup>1</sup>

<sup>1</sup>Department of Hematology, Qilu Hospital, Shandong University, Jinan 250012, China; <sup>2</sup>Shandong Academy of Occupational Health and Occupational Medicine, 18877 Jingshi Road, Jinan 250062, China

Received April 27, 2018; Accepted July 29, 2018; Epub August 15, 2018; Published August 30, 2018

**Abstract:** Objective: Acute myeloid leukemia (AML) is a hematological disease which has been associated with long-term exposure to benzene (BZ) vapors. To develop an animal model of secondary leukemia, BZ can be used as leukemogenic agent. Despite the high frequency of AML is observed in human cases of occupational exposure to BZ, but not commonly observed in mice. Moreover, the association between the BZ exposure and the cause of AML remained incomplete. Methods: We used the CBA/Ca mouse as a model, exhibited a susceptible to AML, allowing investigation into the immunotoxicity effects associated with benzene-induced acute leukemia. Results: Body weight was decreased significantly after 8 weeks BZ exposure in the BZ-acute myeloid leukemia (BZ-AML) group compared with the control group. After 8 weeks of BZ exposure, the BZ-AML model group was associated with an enlarged liver and spleen. Furthermore, molecular studies demonstrated that BZ-induced acute leukemia was closely linked to NLRP3 overexpression, which was in response to impaired immune function. Thus, the CBA/Ca mouse can provide an excellent model for the development of therapeutic strategies against BZ-induced leukemia and allow for study of the molecular etiology in more depth. Conclusions: We developed a BZ-induced AML model in CBA/Ca mice with bone marrow immunophenotypic features.

**Keywords:** Acute myeloid leukemia, benzene, hematopoietic neoplasms, immune function

## Introduction

Benzene (BZ), a well-known leukemogenic agent and has been associated with acute myeloid leukemia (AML), particularly at high exposure concentrations [1, 2]. Long-term exposure to BZ has been shown to increase the incidence of AML in humans [3].

The association between chronic BZ exposure and leukemia in humans has been reported in epidemiological studies [4]. As reported in previous literature, BZ and its metabolites induce hematopoietic toxicity, which is characterized by the induction of aplastic anemia, myelodysplastic syndrome, and leukemia [5]. However, to date, the mechanism by which BZ-induced leukemia (BZ-AML) has not been fully elucidated. In recent years, animal models of BZ exposure have helped to strengthen our understanding of the mechanisms of BZ-induced leukemia [6]. The progression of BZ-AML and its toxic mechanisms are still not known. Previous

research have shown that CBA mouse was susceptible to AML [7], so we used the CBA/Ca mouse in this study and would like to provide an effective treatment protocol.

The involvement of the BZ hematotoxicity mechanism has not yet been clarified. The probable toxic mechanisms of BZ-AML involved the induction of oxidative stress, the dysregulation of cell cycle, the alternation apoptosis of hematopoietic stem cell (HSC), and abnormal proliferation and differentiation of HSC [8, 9]. However, the understanding of leukemogenic mechanisms still remains incomplete. Identification of fundamental underlying mechanisms is an important goal in the risk estimation for the human exposure to BZ.

The precise mechanism of BZ and BZ metabolism toxicity in humans is not perfectly understood, mainly for two reasons: the low natural incidence of AML both in humans and experimental animals, and the association between

## Molecular etiology of BZ-induced hematopoietic neoplasms

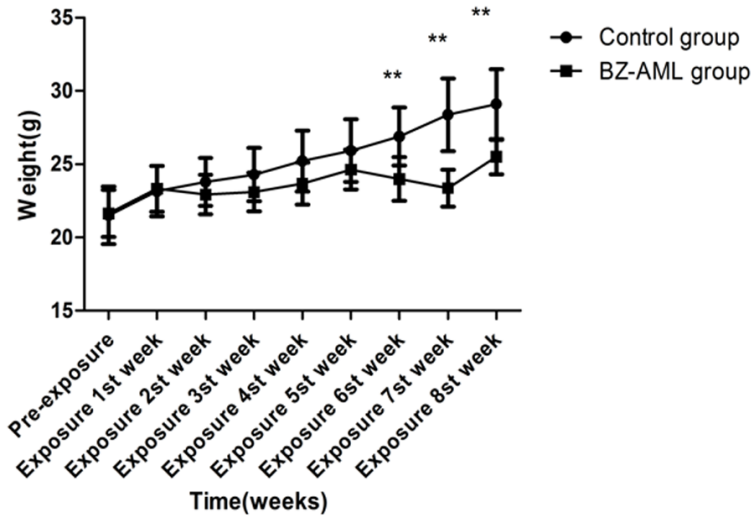


**Figure 1.** Body weight of CBA/Ca mice at different time points. The body weights were monitored each week. Values are expressed as mean  $\pm$  standard deviation (SD). Control: n=10; benzene-induced acute myeloid leukemia (BZ-AML): n=10. (\* $P$ <0.05 \*\* $P$ <0.01 compared with control).

studies have been performed in mice. Kanokporn Rithidech et al. (1999) and Manas Kumar Mukhopadhyay (2013) established BZ-AML in CBA/Ca Swiss albino mice exposed to BZ vapors for 2-16 weeks [10, 11]. The CBA/Ca mouse strain is an excellent animal for the study of leukemogenesis [12, 13]. On the other hand, CBA/Ca mice have been known to be more susceptible to BZ [14, 15]. However, there remain some gaps among the experimental animal studies of BZ-induced leukemias in this field.

In the present study, we exposed mice to BZ for 8 weeks and then investigated the apoptosis rate, cell cycle of bone marrow cells in BZ-exposed mice. The best characterized inflammasome is the NLRP3 (also known as NALP3 and cryopyrin). Although NLRP3 inflammasome has been implicated as essential in the pathogenesis of autoimmune and inflammatory diseases, the role it serves in the development of AML following BZ exposure remains unknown. In this study, the NLRP3 inflammasome expression was investigated and build a successful aim to elucidate the molecular etiology of benzene induced leukemia.

These results suggest that NLRP3 inflammasome may be activated in response to BZ stimuli and may play roles in the development of BZ-induced AML.

### Materials and methods

#### Animals and BZ exposure

A total of 20 male CBA/Ca mice (6-8-weeks-old, purchased from Shanghai Xipuer-Bikai Laboratory Animal Company, SCXK2013-0016) were used for the study. The animals were

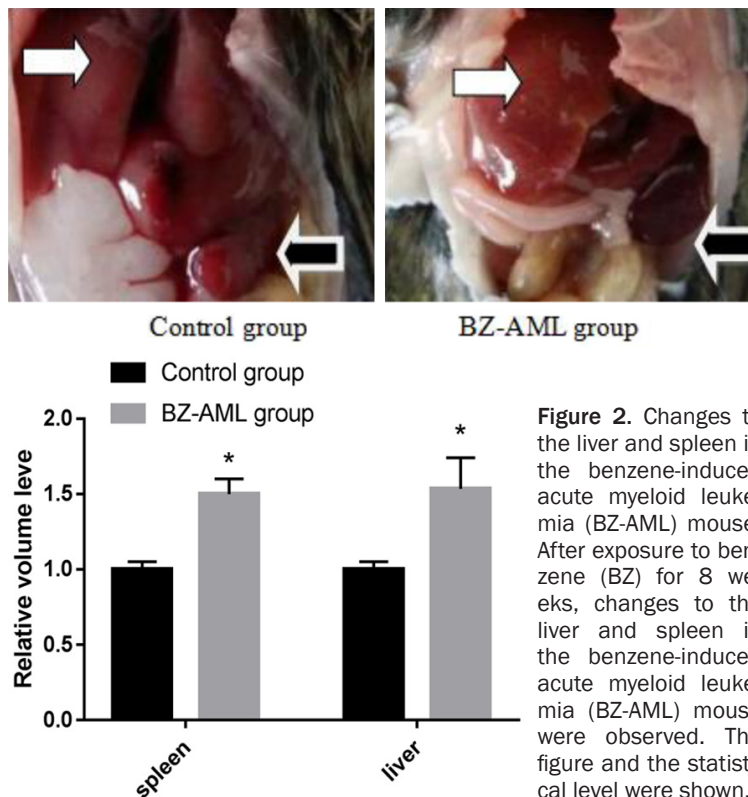


**Figure 2.** Changes to the liver and spleen in the benzene-induced acute myeloid leukemia (BZ-AML) mouse. After exposure to benzene (BZ) for 8 weeks, changes to the liver and spleen in the benzene-induced acute myeloid leukemia (BZ-AML) mouse were observed. The figure and the statistical level were shown.

high and low doses of BZ exposure and the incidence of AML remain unclear. Thus, having an available and appropriate BZ-induced AML (BZ-AML) model is crucial in the production of a mechanistic study and development of an effective treatment protocol. Recently, some

## Molecular etiology of BZ-induced hematopoietic neoplasms

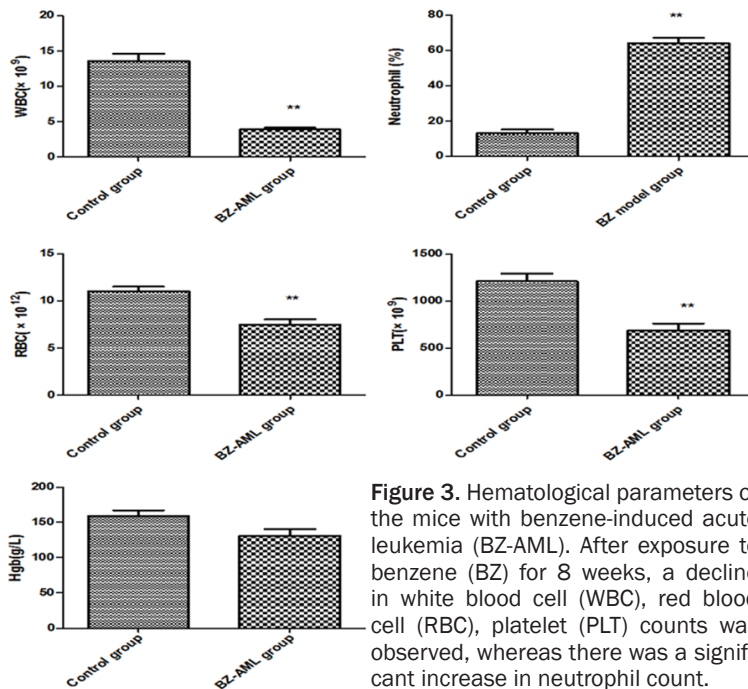


**Figure 3.** Hematological parameters of the mice with benzene-induced acute leukemia (BZ-AML). After exposure to benzene (BZ) for 8 weeks, a decline in white blood cell (WBC), red blood cell (RBC), platelet (PLT) counts was observed, whereas there was a significant increase in neutrophil count.

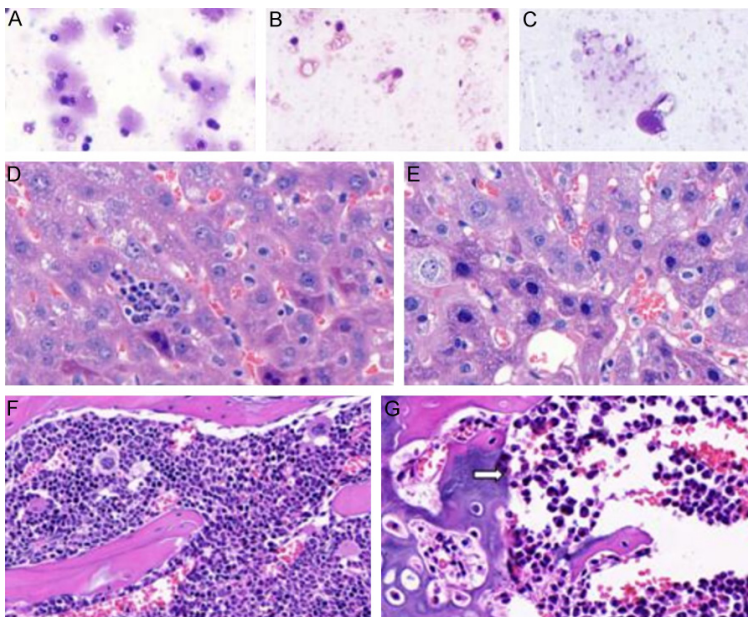


**Figure 4.** Representative histopathological findings for acute myeloid leukemia (AML) development in benzene (BZ)-exposed CBA/CA mice. Typical bone marrow (BM) smears of control (A) and BZ model mice (B). Atypical myeloid cells with scattered bizarrely-shaped myeloblastic nuclei including megakaryocytes (C). A hepatic cell cord filled with an atypical mononuclear myeloblastic cell component surrounding a central vein with hepatic steatosis (D, E). AML in femoral BM (F, G) and its periosteal, intramuscular expansion, and infiltration into the growth surrounding the soft part of the femoral bone.

weighed and placed in stainless steel wire cages (five mice per cage). Food and water was

provided *ad libitum*. The 20 mice were randomly assigned to two different groups, a BZ-AML experimental group, where 10 mice were exposed to 300 ppm of BZ for 6 h per day, 5 d per week for 8 weeks in 0.5 m<sup>3</sup> inhalation chambers (Hope-Med 8050H Equipment, China), or into a control group where 10 mice were exposed to ambient air for the same duration, and interval periods. The BZ concentration in the chambers was monitored at 2 h intervals during daily exposure using an aerosol particle spectrometer (Hope-Med 8050CLA Equipment, China). The temperature and humidity in the chamber were automatically maintained at 23±1°C and (55±10)%, respectively.

### Analysis of diseased mice

To determine the progression of the disease, mice that received BZ exposure were evaluated daily for symptoms of the disease. Disposal of animals during experimental procedures conformed to standard guidelines for laboratory animals.

### BZ and metabolites were analyzed by SPE-GC-MS

Two days after stopping BZ exposure, the animals were weighed, anesthetized with 10% chloral hydrate, and their blood was subsequently removed by cardiac puncture. Whole blood was drawn from punctured hearts and collected in EDTA tubes. Livers, kidneys, spleens, and femurs were isolated. The livers, kidneys, and spleens were perfused with saline to remove any contaminating blood prior to homogenization. BZ

and metabolites were analyzed by SPE-GC-MS (A method based on solid-phase extraction and

## Molecular etiology of BZ-induced hematopoietic neoplasms

**Table 1.** Concentrations of BZ metabolites in different tissues analyzed by SPE-GC-MS ( $\mu\text{g/g}$ )

Tissue	Group	BZ	P	CAT	HQ	BT
Blood	Control	0.3±0.26	0.18±0.10	0.40±0.28	0.38±0.35	1.12±0.93
	BZ-AML	7.07±0.99**	9.9±2.31**	343.59±141.37**	33.77±30.33**	188.24±38.64**
Marrow	Control	0.13±0.16	1.11±0.12	2.11±0.71	0.22±0.14	37.73±16.95
	BZ-AML	0.34±0.19*	10.74±5.09**	73.22±27.01**	1.96±0.13*	167.70±115.71**
Kidney	Control	0.07±0.03	0.07±0.02	0.27±0.14	0.23±0.27	5.94±1.94
	BZ-AML	0.16±0.04*	0.51±0.36**	15.68±4.11**	2.33±0.93**	20.93±2.43**
Spleen	Control	0.15±0.02	0.80±0.06	1.53±0.41	0.14±0.09	0.96±1.52
	BZ-AML	2.11±0.64**	3.72±0.33**	31.43±24.09**	15.63±7.60**	22.74±6.93**
Liver	Control	0.05±0.04	0.25±0.06	0.10±0.04	0.11±0.05	6.54±3.25
	BZ-AML	2.87±2.21**	1.16±0.08*	2.28±0.28**	1.63±0.25**	19.71±6.18**

Values are expressed as mean  $\pm$  SD (n=3) for all samples. HQ, hydroquinone; P, phenol; CAT, catechol; BZ, benzene, BT, benzenetriol. \*P<0.05, \*\*P<0.001.

subsequent analysis by gas chromatography combined with mass spectrometry [16].

### *Hematological parameters, blood, and bone marrow (BM) smears*

After completion of the experiment, approximately 20  $\mu\text{L}$  peripheral blood was collected by tail vein puncture from each animal using EDTA-K2-containing tubes for the cell count. Total and differential white blood cell (WBC) counts, red blood cell (RBC) counts, platelet (PLT) counts, and hemoglobin (HGB) levels were analyzed fresh on a hematology analyzer BC-2800-Vet (Mindray, China).

### *Flow cytometry analysis*

For detection of bone marrow mononuclear cells (BMMNC) apoptosis, we used an Annexin V-FITC apoptosis detection kit (Jinmei Biotech Co, China) and propidium iodide (PI) double staining, as well as flow cytometry. Cells were harvested, washed twice with cold PBS, and resuspended at  $1 \times 10^6$  cells/mL in  $1 \times$  binding buffer, Annexin V-FITC (5  $\mu\text{L}$ ), and PI (5  $\mu\text{L}$ ) were added to the PBS (100  $\mu\text{L}$ ) in the dark followed by incubation for 15 min at 4°C, and flow cytometry (Beckman Coulter, USA) was conducted within 1 h. Data analysis was performed using Kaluza Flow Cytometry software.

Cells ( $10^6$ ) were fixed in ice-cold 70% ethanol at 4°C for 12 h, washed with cold PBS, collected, and resuspended in DNA staining solution (Solarbio, Beijing, China) for 30 min in the dark at room temperature. DNA content was analyzed by using a CytoFLEX flow cytometer and

CellQuest software (Beckman Coulter, USA). Cell cycle distribution was analyzed with ModFit LT 3.1 software (Verity Software House, ME, USA).

### *Immunohistochemistry (IHC)*

Bone marrow samples were embedded in paraffin and cut into 5  $\mu\text{m}$  sections. Detection of NLRP3 was performed. Tissue sections were exposed overnight to rabbit anti-NLRP3 antibody (Servicebio INC, USA) at 4°C, washed in PBS and then incubated with biotinylated goat anti-rabbit for 50 min at 37°C. Sections visualized with DAB staining and were analyzed using Image-Pro Plus version 6.0 (MediaCybernetics, Inc, MD). The result was expressed as the ratio of positive to negative (brown-yellow) staining area.

### *Statistical analysis*

All the values are presented as mean  $\pm$  standard deviation. Statistical analysis was performed in GraphPad Prism version 5.01 for Windows (Graph-Pad Software, San Diego California USA). Differences between the BZ-AML group and the control group were analyzed with Student's t-test. Differences were considered as significant at P<0.05 level.

## Results

### *Body weight and enlarged liver and spleen*

Body weight decreased significantly from sixth week after BZ exposure in the BZ-AML group compared to the control group (**Figure 1**). The alternations became more pronounced with

Molecular etiology of BZ-induced hematopoietic neoplasms

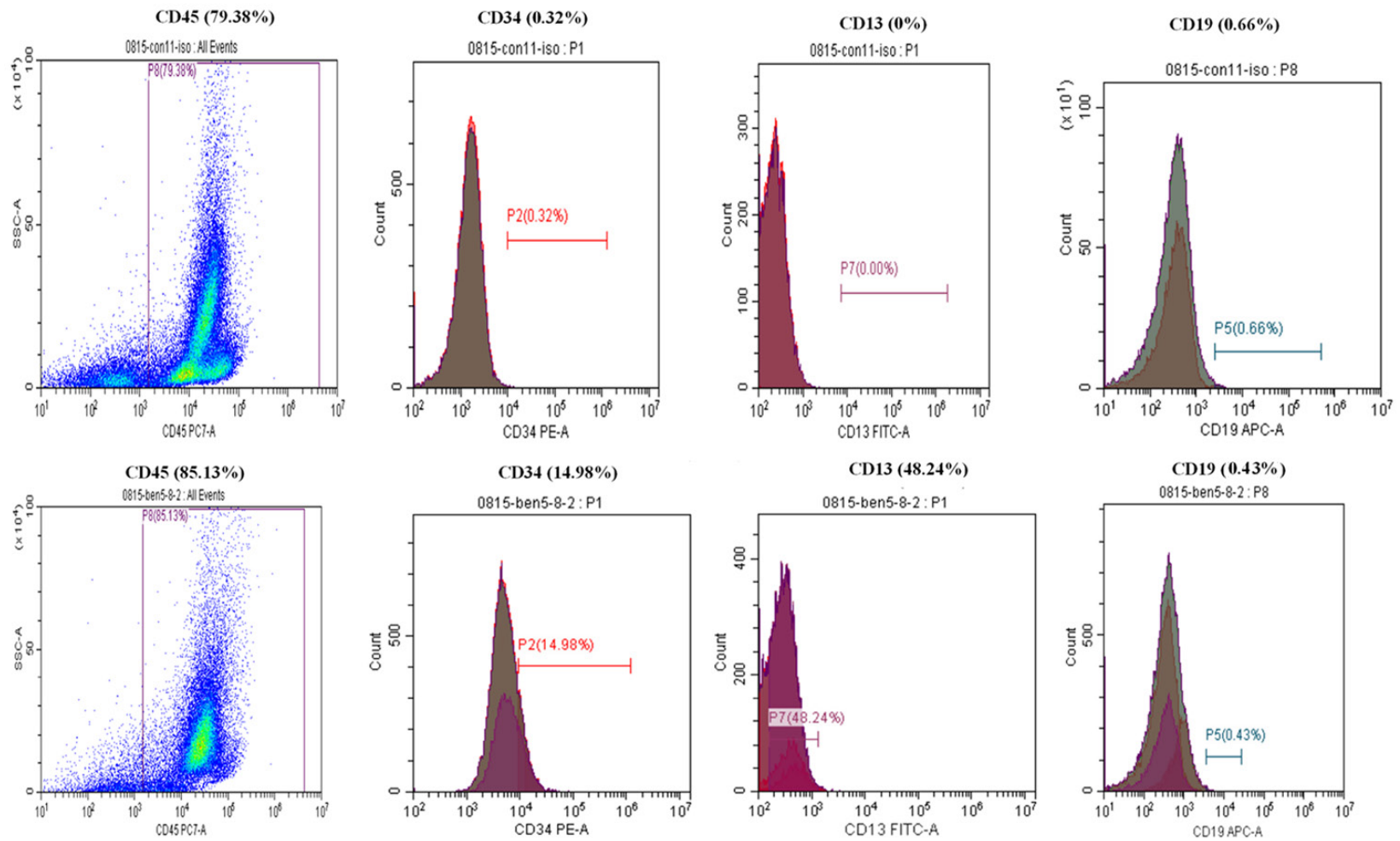


**Figure 5.** Flow cytometry results using mice-specific antibodies showing the CD45<sup>+</sup>CD34<sup>+</sup>CD13<sup>+</sup>CD19<sup>-</sup> immunophenotype in bone marrow of the BZ-AML and control groups.

## Molecular etiology of BZ-induced hematopoietic neoplasms

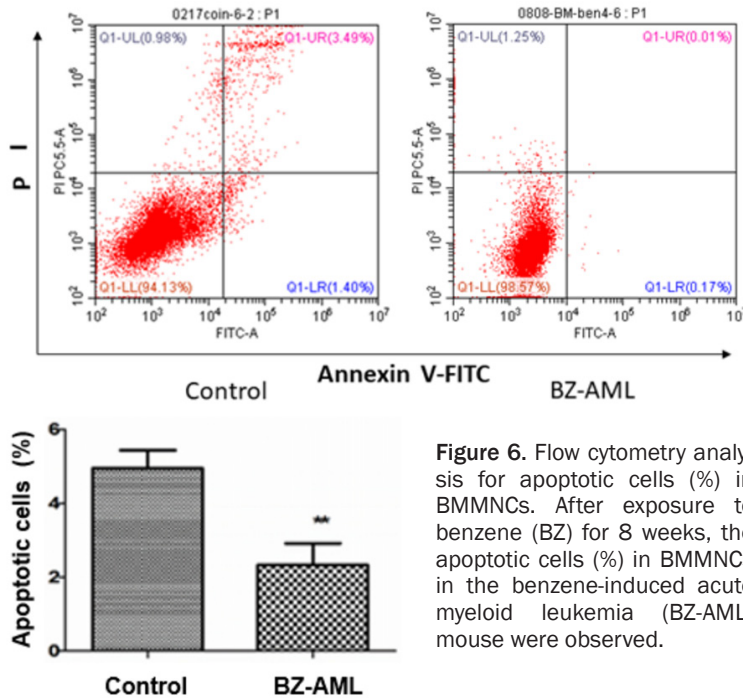


**Figure 6.** Flow cytometry analysis for apoptotic cells (%) in BMMNCs. After exposure to benzene (BZ) for 8 weeks, the apoptotic cells (%) in BMMNCs in the benzene-induced acute myeloid leukemia (BZ-AML) mouse were observed.

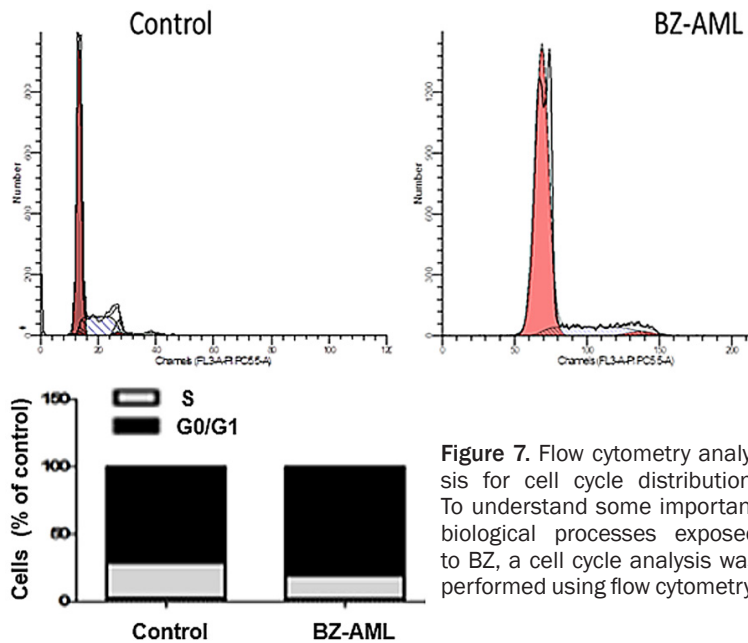


**Figure 7.** Flow cytometry analysis for cell cycle distribution. To understand some important biological processes exposed to BZ, a cell cycle analysis was performed using flow cytometry.

increasing exposure duration. After 8 weeks of BZ exposure, the BZ-AML model group was associated with an enlarged liver and spleen (Figure 2).

### Hematological parameters, blood, and BM smear analysis

Hematological parameters of the mice with benzene-induced acute leukemia (BZ-AML)

were analyzed. After exposure to benzene for 8 weeks, Hematological parameters of the mice show that there was a decline in WBC, RBC, and PLT counts, while there was a significant increase in neutrophil count (Figures 3 and 4).

### Analysis of BZ and its metabolites by SPE-GC-MS

In the BZ-AML group and control group, Benzene and its metabolites were analyzed by SPE-GC-MS. After exposing to Benzene, Benzene level in blood of control group is different from that of BZ-AML group, and the difference was statistically significant ( $P < 0.05$ ), while in the Marrow, Kidney, Spleen and Liver, the level of Benzene metabolites is different in BZ-AML group from that in BZ-AML group and the difference was statistically significant ( $P < 0.01$ ). Benzene toxicity involves both bone marrow depression and leukemogenesis caused by damage to multiple classes of hematopoietic cells and a variety of hematopoietic cell functions. Benzene is metabolized, primarily in the liver, to a variety of hydroxylated and ring-opened products that are transported to the bone marrow where subsequent secondary metabolism occurs. The results shows that several metabolites of benzene play significant roles in generating benzene toxicity. (Table 1).

### Flow cytometry analysis with mice-specific antibodies shows a myeloid progenitor immunophenotype ( $CD45^+CD34^+CD13^+CD19^-$ ) in bone marrow.

After exposure to BZ for 8 weeks, the BZ-AML model group showed a myeloid progenitor immunophenotype  $CD45^+CD34^+CD13^+$  in the bone marrow of the BZ-AML group.  $CD34^+$  myeloid cells in the BZ-AML group made up 14.98% of the total cell count, and this was

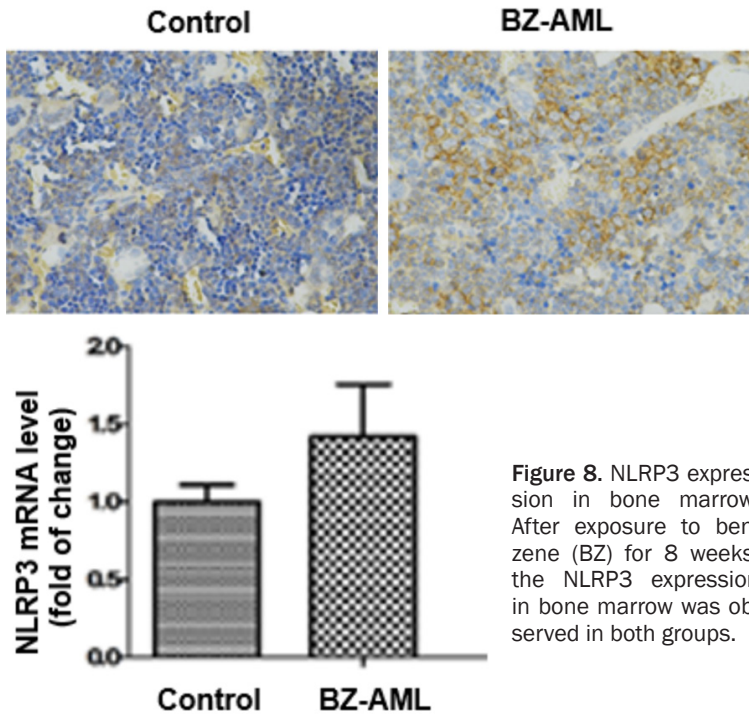


**Figure 8.** NLRP3 expression in bone marrow. After exposure to benzene (BZ) for 8 weeks, the NLRP3 expression in bone marrow was observed in both groups.

*NLRP3 expression in bone marrow*

Immunopositive cells in the bone marrow sections were counted. A significant increase in NLRP3 inflammasome numbers was observed in the BZ-AML mice ( $P < 0.05$ ) (**Figure 8**).

**Discussion**

Long-term inhalation of BZ has been shown to cause hematotoxicity and an increased incidence of AML in humans [17]. The progression of BZ-induced hematotoxicity and how this toxicity plays a major role in the leukemogenesis are not known [18]. In the present study, we presented the hematological consequences of BZ inhalation in CBA/CA mice

exposed to 300 ppm BZ for for 8 weeks (6 h/day \* 5 d/week).

The mouse AML model recapitulates the phenotypic and molecular genetic features of primary human AML [19]. This murine model could be used to evaluate the therapeutic strategies for treatment of AML [20, 21]. In this study, we showed that weight was decreased significantly after 6 weeks post BZ exposure. These alternations became more pronounced with increasing exposure duration. After 8 weeks of BZ exposure, the mice in the BZ-AML model group became associated with an enlarged liver and spleen. Mirroring these results, mice exposed to BZ were more prone to changes in body weight and also in the liver and spleen.

According to our results, following exposure to BZ for 8 weeks, there was a decline in WBC, RBC, and PLT counts, whereas there was a significant increase in the neutrophil count, these abnormal parameters are similar to that of AML.

Flow cytometry analysis of the bone marrow showed that mice had a CD45<sup>+</sup>CD34<sup>+</sup>CD13<sup>+</sup>CD19<sup>-</sup> immunophenotype, which is consistent with the observations from DEK-NUP-214-transduced CD34<sup>+</sup> cells in the NSG-SGM3 mouse model [22].

higher than that of the control group (0.32% of the total cell count). The percentage of CD13<sup>+</sup> myeloid cells in the BZ-AML group was 48.24% and this was higher than that of the control group, where the percentage was 0% (**Figure 5**).

*Flow cytometry analysis for apoptotic cells (%) in BMMNCs*

Annexin-V/PI method can distinguish between two kinds of apoptotic BMMNC cells. Annexin-V<sup>+</sup>/PI<sup>+</sup> are referred as late apoptotic cell populations and Annexin-V<sup>+</sup>/PI<sup>-</sup> as early apoptotic cells. Apoptotic cells composed of Annexin-V<sup>+</sup>/PI<sup>+</sup> and Annexin-V<sup>+</sup>/PI<sup>-</sup> apoptotic cell populations. At the end of 8 week BZ exposure, we observed a significant decrease in BMMNC apoptotic cells of (2.34±1.85)% in BZ-AML group, compared with the control group of (4.96±1.51)% ( $p < 0.01$ ) (**Figure 6**).

*Flow cytometry analysis for cell cycle distribution*

To understand some important biological processes exposed to BZ, a cell cycle analysis was performed using flow cytometry. And G0/G1 arrest was observed in BZ-AML group ( $p < 0.05$ ) (**Figure 7**).

Inflammasomes are vital players in innate immunity. It is associated with onset and progression of various diseases, including multiple sclerosis, inflammatory bowel disease, as well as other auto-immune and auto-inflammatory diseases. In this study we observed a significant increase in NLRP3 inflammasome numbers in the BZ-AML mice, suggesting that the NLRP3 overexpression plays a role in the pathology of BZ-AML, which is similar to the results of another study [23].

In summary, we successfully established the BZ-induced AML model in CBA/Ca mice. Our results suggest that, upregulation of CD34<sup>+</sup> and CD13<sup>+</sup> correlates with BZ-induced AML.

### Acknowledgements

This work was supported by the National Natural Science Foundation of China (9164-2110, 81470319) and the Natural Science Foundation of Shandong Province (ZR2017-BH088).

### Disclosure of conflict of interest

None.

**Address correspondence to:** Dr. Min Ji, Department of Hematology, Qilu Hospital, Shandong University, 107 West Wenhua Road, Jinan 250012, China. Tel: +8618560087026; E-mail: jimmin@sdu.edu.cn

### References

- [1] Peng C and Ng JC. The role of epigenetic changes in benzene-induced acute myeloid leukaemia. *J Clin Epigenetics* 2016; 2: 19.
- [2] Wei C, Chen M, You H, Qiu F, Wen H, Yuan J, Xiang S and Yang X. Formaldehyde and co-exposure with benzene induce compensation of bone marrow and hematopoietic stem/progenitor cells in BALB/c mice during post-exposure period. *Toxicol Appl Pharmacol* 2017; 324: 36-44.
- [3] Gashev AA and Zawieja DC. Lymph transport and lymphatic system. *Encyclopedia of Immunotoxicology* 2016; 547-549.
- [4] Yaris F, Dikici M, Akbulut T, Yaris E and Sabuncu H. Story of benzene and leukemia: epidemiologic approach of muzaffer aksoy. *J Occup Health* 2004; 46: 244-247.
- [5] Snyder R. Overview of the toxicology of benzene. *J Toxicol Environ Health A* 2000; 61: 339-346.
- [6] Rithidech K, Dunn JJ, Bond VP, Gordon CR and Cronkite EP. Characterization of genetic instability in radiation- and benzene-induced murine acute leukemia. *Mutat Res* 1999; 428: 33-39.
- [7] Silver A and Cox R. Telomere-like DNA polymorphisms associated with genetic predisposition to acute myeloid leukemia in irradiated CBA mice. *Proc Natl Acad Sci U S A* 1993; 90: 1407-1410.
- [8] AbdulSalam SF, Thowfeik FS and Merino EJ. Excessive reactive oxygen species and exotic DNA lesions as an exploitable liability. *Biochemistry* 2016; 55: 5341-5352.
- [9] Hernández AF and Menéndez P. Linking pesticide exposure with pediatric leukemia: potential underlying mechanisms. *Int J Mol Sci* 2016; 17: 461.
- [10] Kawasaki Y, Hirabayashi Y, Kaneko T, Kanno J, Kodama Y, Matsushima Y, Ogawa Y, Saitoh M, Sekita K and Uchida O. Benzene-induced hematopoietic neoplasms including myeloid leukemia in trp 53-deficient C57BL/6 and C3H/He mice. *Toxicol Sci* 2009; 110: 293-306.
- [11] Mukhopadhyay MK and Nath D. Physiologically based toxicokinetic modeling of secondary acute myelolytic leukemia. *Environ Toxicol Pharmacol* 2014; 37: 378-389.
- [12] Young NS. Acquired aplastic anemia. *Ann Intern Med* 2002; 136: 534-546.
- [13] Das M, Chaudhuri S and Law S. Benzene exposure-An experimental machinery for induction of myelodysplastic syndrome: stem cell and stem cell niche analysis in the bone marrow. *J Stem Cells* 2012; 7: 43-59.
- [14] Maiborodin I, Agzaev M, Ragimova T and Maiborodin I. Age-related changes in the structure of lymphoid organs: a review of the literature. *Adv Gerontol* 2016; 6: 282-290.
- [15] Karthik R, Vinoth Kumar J, Chen SM, Karupiah C, Cheng YH and Muthuraj V. A study of electrocatalytic and photocatalytic activity of cerium molybdate nanocubes decorated graphene oxide for the sensing and degradation of antibiotic drug chloramphenicol. *ACS Appl Mater Interfaces* 2017; 9: 6547-6559.
- [16] Li H, Jiang Z, Cao X, Su H, Shao H, Jin F, Zheng L, El-Aty AA and Wang J. SPE/GC-MS determination of 2-pyrrolidone, N-methyl-2-pyrrolidone, and N-ethyl-2-pyrrolidone in liquid pesticide formulations. *Chromatographia* 2018; 81: 359-364.
- [17] Linet MS, Yin SN, Gilbert ES, Dores GM, Hayes RB, Vermeulen R, Tian HY, Lan Q, Portengen L and Ji BT, Li GL, Rothman N; Chinese Center for Disease Control and Prevention-U.S. National Cancer Institute Benzene Study Group. A retrospective cohort study of cause-specific mortality and incidence of hematopoietic malignancies in Chinese benzene-exposed workers. *Int J Cancer* 2015; 137: 2184-2197.

## Molecular etiology of BZ-induced hematopoietic neoplasms

- [18] Snyder R and Hedli CC. An overview of benzene metabolism. *Environ Health Perspect* 1996; 104 Suppl 6: 1165-71.
- [19] Abarrategi A, Mian SA, Passaro D, Rouault-Pierre K, Grey W and Bonnet D. Modeling the human bone marrow niche in mice: from host bone marrow engraftment to bioengineering approaches. *J Exp Med* 2018; 215: 729-743.
- [20] Maertens O, McCurrach ME, Braun BS, De Raedt T, Epstein I, Huang TQ, Lauchle JO, Lee H, Wu J and Cripe TP. A collaborative model for accelerating the discovery and translation of cancer therapies. *Cancer Res* 2017; 77: 5706-5711.
- [21] Gu R, Wei H, Wang Y, Lin D, Liu B, Zhou C, Liu K, Gong B, Wei S and Zhang G. The number of CD34<sup>+</sup> CD38<sup>+</sup> CD117<sup>+</sup> HLA-DR<sup>+</sup> CD13<sup>+</sup> CD33<sup>+</sup> cells indicates post-chemotherapy hematopoietic recovery in patients with acute myeloid leukemia. *PLoS One* 2017; 12: e0180624.
- [22] Qin H, Malek S, Cowell JK and Ren M. Transformation of human CD34<sup>+</sup> hematopoietic progenitor cells with DEK-NUP214 induces AML in an immunocompromised mouse model. *Oncogene* 2016; 35: 5686.
- [23] Jia Y, Zhang C, Hua M, Wang M, Chen P and Ma D. Aberrant NLRP3 inflammasome associated with aryl hydrocarbon receptor potentially contributes to the imbalance of T-helper cells in patients with acute myeloid leukemia. *Oncol Lett* 2017; 14: 7031-7044.